

# Defects in the $(\sqrt{3}\times\sqrt{3})\Leftrightarrow(3\times 3)$ phase transition in the Pb/Si(111) system

I. Brihuega,<sup>1,\*</sup> O. Custance,<sup>2</sup> M. M. Ugeda,<sup>1</sup> and J. M. Gómez-Rodríguez<sup>1</sup>

<sup>1</sup>*Departamento Física de la Materia Condensada, Universidad Autónoma de Madrid, E-28049 Madrid, Spain*

<sup>2</sup>*Graduate School of Engineering, Osaka University, 2-1 Yamada-Oka, Suita, Osaka 565-0871, Japan*

(Received 22 December 2006; published 11 April 2007)

The role played by point defects in the  $(\sqrt{3}\times\sqrt{3})\Leftrightarrow(3\times 3)$  phase transition that takes place in the 1/3 monolayer-Pb/Si(111) system has been investigated by means of variable temperature scanning tunneling microscopy. In this system, it has been possible to grow exceptionally large defect-free regions coexisting with more defective ones. These defective regions have between 2% and 5% of point defects, which are mainly substitutional Si adatoms. Our experiments show that the point defects produce a local perturbation of the surface, but discard them as the fundamental driving force of the phase transition. By tracking exactly the same surface regions with atomic resolution while varying the sample temperature from 40 to 200 K, we have observed that substitutional point defects are not mobile throughout the phase transition and our statistical analysis of the STM images reveals that they are randomly placed from 40 K to room temperature.

DOI: [10.1103/PhysRevB.75.155411](https://doi.org/10.1103/PhysRevB.75.155411)

PACS number(s): 68.35.Rh, 68.35.Bs, 68.37.Ef

## I. INTRODUCTION

The ability to probe the solid surfaces in real space with atomic resolution has recently opened a unique opportunity to deepen our understanding of the physical basis of two-dimensional phase transitions. The particular character of phase transitions in this reduced dimensionality makes them one of the most interesting topics in condensed matter physics. One of the fundamental questions is the role of the ubiquitous defects, which are expected to have a more significant influence than in the three-dimensional case. This general question is particularly relevant to the  $(\sqrt{3}\times\sqrt{3})R30^\circ\Leftrightarrow(3\times 3)$  reversible phase transition that takes place in the family of systems formed by the adsorption of 1/3 monolayer (ML) Pb or Sn on Ge(111) and 1/3 ML Pb on Si(111) surfaces,<sup>1-3</sup> where, in spite of the extensive experimental and theoretical work performed,<sup>1-17</sup> the role played by defects is still a widely debated subject.<sup>5,8,15,18-20</sup>

At room temperature (RT), these isovalent systems present a surface with a  $(\sqrt{3}\times\sqrt{3})R30^\circ$  (referred to as  $\sqrt{3}$  in the following) periodicity, which evolves to  $(3\times 3)$  at low temperature (LT). The study of this temperature-mediated phase transition has been faced with many different experimental and theoretical approaches, but its origin and the physical mechanisms responsible for it are still controversial [very recently, even the widely accepted belief that the ground state at the lowest temperatures was the  $(3\times 3)$  phase has been challenged by some authors for the 1/3 ML Pb and Sn on Ge(111) systems<sup>15,20,21</sup>]. One of the main difficulties when investigating the  $\sqrt{3}\Leftrightarrow(3\times 3)$  phase transition arises from the presence of point defects. Usually these surfaces possess, at least, between 2% and 5% of point defects,<sup>8</sup> which are mainly substitutional substrate atoms, that strongly affect the behavior of the phase transition. In the present work, in order to avoid the presence of these point defects and also to understand the role played by them in the  $\sqrt{3}\Leftrightarrow(3\times 3)$  phase transition, our system of choice has been the Pb/Si(111) interface, where we have been able to grow very large defect-free regions that coexist with more defective ones.<sup>3</sup> This special morphology of our surfaces has allowed us to discern between the intrinsic character of the

phase transition and the influence of the substitutional defects on it. Measuring bias voltage dependent scanning tunneling microscopy (STM) images, we have identified the nature of point defects, studied the local perturbation generated from the point defects, and finally, investigated the possible existence of the motion of these defects in the vicinity of the phase transition due to a defect-defect interaction with the  $(3\times 3)$  periodicity.

## II. EXPERIMENTAL DETAILS

The experiments were carried out in an ultrahigh vacuum (UHV) system whose base pressure is below  $5\times 10^{-11}$  Torr. The system is equipped with a homemade ultrastable variable temperature STM (VT-STM), which allows imaging at sample temperatures in the range of 40–400 K,<sup>22,23</sup> low-energy electron diffraction (LEED), Auger electron spectroscopy, sample and STM tip transfer and heating capabilities, a STM tip cleaning system by field emission, several interchangeable evaporation cells, a quartz crystal microbalance, and an ion gun for sample cleaning purposes.

In order to obtain large defect-free regions, it was necessary to prepare the samples in a very careful way. Our sample preparation method consisted in depositing at RT  $\sim 1$  ML Pb on top of a clean Si(111)- $7\times 7$  surface, obtained by flashing the sample at  $\sim 1150^\circ\text{C}$  followed by a slow cooling down to RT. Subsequently, Pb was desorbed by annealing the sample at  $\sim 450^\circ\text{C}$  (Ref. 24) for several minutes until a final coverage of  $\sim 0.6$ – $0.7$  ML Pb was obtained. Then, LEED was always performed to check the sample state. We were able to associate the desired surface morphology with a very specific LEED pattern, in which the spots corresponding to the  $\sqrt{3}$  periodicity have a very weak intensity (see Fig. 1). Thus, only if the LEED pattern was the appropriate one will the sample be transferred to the STM, where it was slowly cooled down to the desired temperature. This preparation procedure leads to the formation of surfaces presenting at LT a coexistence of  $(\sqrt{7}\times\sqrt{3})$ -Pb islands with  $(3\times 3)$ -Pb domains.<sup>10,25</sup> The  $(\sqrt{7}\times\sqrt{3})$ -Pb phase is stable up to temperatures of 250 K, where it experiences a different phase transition.<sup>26,27</sup>

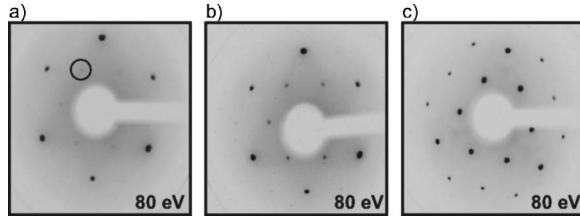


FIG. 1. LEED patterns measured at RT in the Pb/Si(111) system. (a) LEED pattern corresponding to a sample with  $\sim 0.6\text{--}0.7$  ML Pb coverage. These samples present the desired large defect-free regions. The key point is the very weak intensity of the  $\sqrt{3}$  symmetry peaks (the position of one  $\sqrt{3}$  peak is outlined by a circle). (b) LEED pattern characteristic of a sample with  $\sim 1/3$  ML Pb coverage. The  $\sqrt{3}$  regions of such samples have a higher Si defect density compared to  $\sqrt{3}$  regions in (a). (c) LEED pattern corresponding to a sample with  $\sim 1/6$  ML Pb coverage. These surfaces present a mosaic phase ( $\sim 50\%$  of substitutional Si adatoms).

### III. RESULTS AND DISCUSSION

#### A. Description of the $(\sqrt{3}\times\sqrt{3})\leftrightarrow(3\times 3)$ phase transition in the Pb/Si(111) system

In this work, our experiments have been focused on the  $1/3$  ML Pb/Si(111) phase. It has been reported that this phase experiences a second-order structural phase transition from a  $\sqrt{3}$  symmetry at RT to a  $(3\times 3)$  at  $T_c\sim 86$  K.<sup>3</sup> STM

images obtained above  $T_c$  show, at both polarities, an apparently flat surface where all the lead atoms appear equivalent and arranged in a  $\sqrt{3}$  hexagonal lattice [Figs. 2(c) and 2(e)]. At LT while occupied state STM images show a corrugated surface where one out of three lead atoms of the unit cell appears brighter and arranged in a hexagonal  $(3\times 3)$  lattice [Fig. 2(d)], empty state STM images also show a corrugated surface but with the lead atoms' intensity inverted, i.e., the Pb atoms which appeared brighter in occupied state images now appear darker. Thus, what is observed in empty state STM images is a honeycomb lattice with  $(3\times 3)$  periodicity [Fig. 2(f)].

“True variable” temperature STM experiments, performed previously by us,<sup>3</sup> have shown the reversible character of this phase transition and have been able to determine a critical temperature  $T_c\sim 86$  K for the large defect-free regions. Moreover, first-principles density-functional theory calculation has shown that the presence of a surface soft phonon is associated with the phase transition<sup>3</sup> in a similar way to that shown for the Sn/Ge(111) system.<sup>9,13,28</sup> Above  $T_c$ , the system is oscillating in a correlated manner [i.e., maintaining locally a  $(3\times 3)$  periodicity] with Pb atoms displaying large vertical displacement of  $\sim 0.3$  Å. The time scale of this dynamical fluctuation is approximately in picoseconds and the STM, which occurs in a time scale of approximately microseconds, measures an average of this oscillation and thus observes all

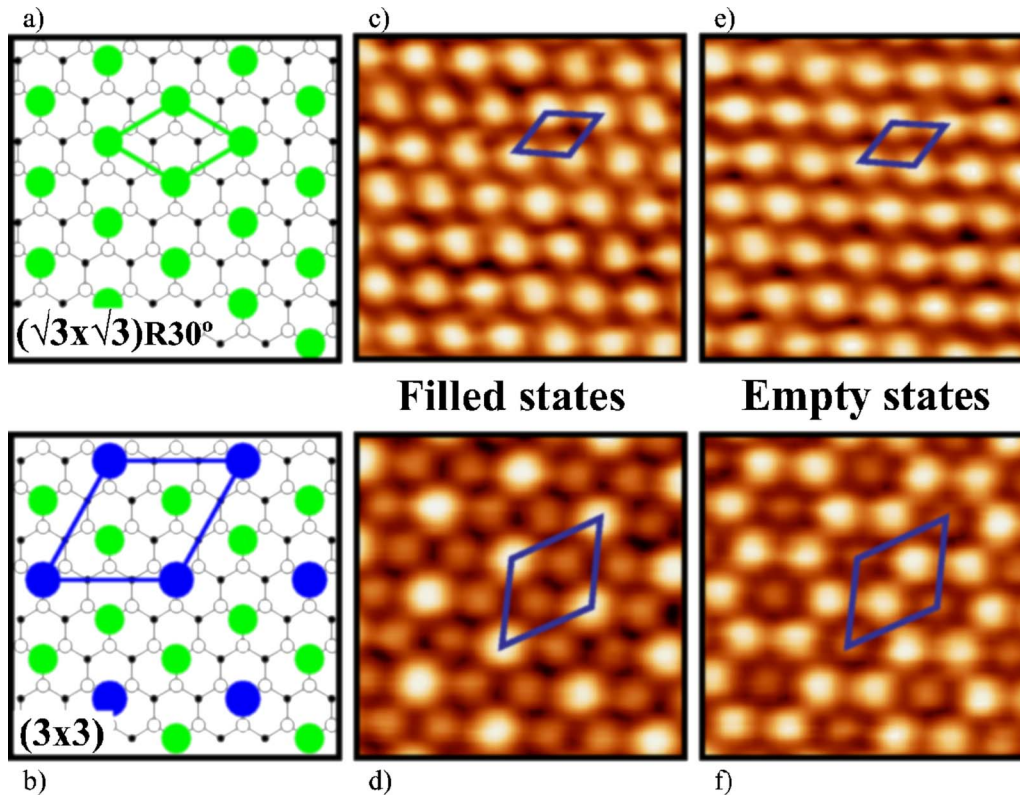


FIG. 2. (Color online) (a) and (b) Schematic atomic models for the  $\sqrt{3}$  and  $(3\times 3)$  phases, respectively. (c)–(f)  $4.0\times 4.0$  nm<sup>2</sup> filled and empty-stated STM images simultaneously measured in the  $1/3$  ML Pb/Si(111) system. Above  $T_c$ , both filled (c) and empty (e) state STM images show a flat surface with a  $\sqrt{3}$  symmetry. Below  $T_c$ , one out of three Pb atoms becomes inequivalent and appears brighter (darker) in filled (d) [empty (f)] state STM images compared to the other two Pb atoms of the unit cell. The STM sample voltages, tunneling currents, and measurement temperatures are (c)  $-0.5$  V, 10 nA, 110 K; (e)  $+0.5$  V, 10 nA, 110 K; (d)  $-0.5$  V, 0.2 nA, 40 K; and (f)  $+0.5$  V, 0.2 nA, 40 K.

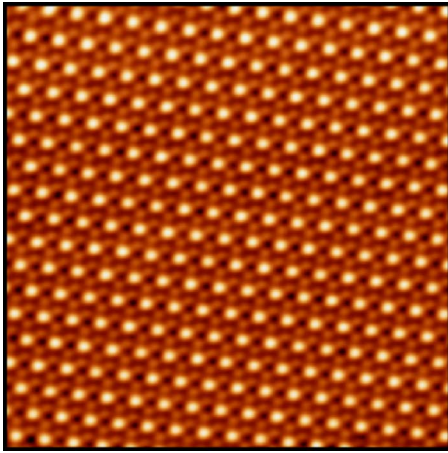


FIG. 3. (Color online) 400 nm<sup>2</sup> STM image showing a completely defect-free region in the 1/3 ML Pb/Si(111) system. The image was measured at 40 K, at a sample bias of  $-1.5$  V, and a tunnel current of 0.1 nA.

the Pb atoms as equivalent with a  $\sqrt{3}$  symmetry. At LT this soft mode freezes in the  $(3\times 3)$  structure. Our recent STM experiments performed at 10 K (Ref. 15) have shown that this  $(3\times 3)$  symmetry is maintained even at such low temperatures, demonstrating that the ground state for the 1/3 ML Pb/Si(111) system at the lowest temperatures is the  $(3\times 3)$  phase.

#### B. Morphology of the 1/3 ML Pb/Si(111) surface: Large defect-free regions and point defect characterization

The existence of defects on real surfaces is unavoidable and the systems where the  $\sqrt{3}\leftrightarrow(3\times 3)$  phase transition takes place are not an exception. In previous works, it has been reported that even in the most favorable cases these surfaces possess between 2% and 5% of point defects.<sup>8</sup> The role played by these defects in the phase transition is controversial, and they have even been considered as responsible for its existence.<sup>6,8,18</sup> In any case, it is clear that the presence of these point defects blurs the intrinsic character of the phase transition. In the Pb/Si(111) system, using the sample preparation procedure described above, we have been able to grow very large defect-free regions that have allowed us to detect the intrinsic character of the phase transition.<sup>3</sup> These defect-free regions can be as large as 400 nm<sup>2</sup>, which is 1 order of magnitude larger than any other defect-free region previously reported in the literature for these types of systems. One example of these extremely large defect-free regions is presented in Fig. 3, in which a  $20\times 20$  nm<sup>2</sup> completely defect-free domain can be observed.

Together with these perfect regions, our Pb/Si(111) surfaces are also composed of more defective ones. In these defective regions, the amount of point defects can vary depending on the final coverage of the sample (given by the annealing time) or the annealing temperature. However, when the surface presents large defect-free regions such as the one shown in Fig. 3, the amount of point defects in the defective regions is between 2% and 5%. By means of bias voltage dependent STM images, two types of point defects

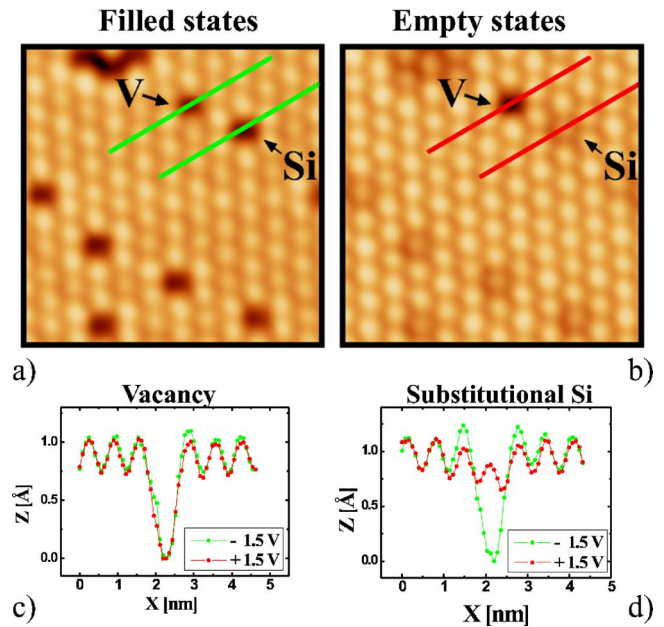


FIG. 4. (Color online) (a) and (b)  $7.0\times 7.0$  nm<sup>2</sup> filled and empty state STM images simultaneously measured at RT in a defective region of the 1/3 ML Pb/Si(111) system. While in the filled state STM image (a) all the point defects appear as dark depressions compared to Pb adatoms, in the empty state STM image (b) only one of them, which corresponds to a vacancy, remains dark as in (a) and the others, which are substitutional Si adatoms, became similar in height compared to the Pb adatoms. (c) and (d) Line profiles along the vacancy (c) and along one of the substitutional Si adatoms (d). Sample voltages and tunnel currents are  $-1.5$  V, 0.2 nA (a) and  $+1.5$  V, 0.2 nA (b).

have been identified: substitutional Si adatoms, which account for 90% of the defects, and vacancies, which represent the remaining 10%. The appearance of substitutional Si defects displays a strong bias voltage dependency, whereas the appearance of vacancies remains almost the same when changing the bias voltage. In occupied state STM images, both the substitutional Si adatoms and vacancies are seen as dark depressions. When measuring empty state STM images, a different scenario is found: while vacancies are still observed as dark depressions, substitutional Si adatoms show similar height compared to Pb adatoms. This can be clearly observed in Figs. 4(a) and 4(b), where two STM images simultaneously measured at  $-1.5$  V (a) and  $+1.5$  V (b) are shown. Together with these STM images, line profiles along the two different types of point defects have been plotted in Figs. 4(c) and 4(d). In these line profiles, it is easily observed that the relative height between vacancies and Pb adatoms remains almost unchanged when varying the bias voltage (c) and how the relative height between substitutional Si adatoms and Pb adatoms becomes similar in empty state images (d). Moreover, as will be discussed later, in occupied states brighter Pb adatoms surrounding substitutional Si defects are detected.

The identification performed about the nature of the two types of point defects is confirmed due to the fact that only the amount of substitutional Si defects is increased when increasing the annealing time, up to a point in which the

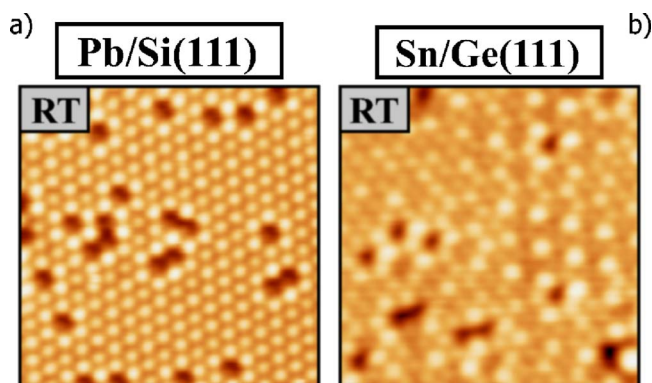


FIG. 5. (Color online) RT STM images of the Pb/Si(111) (a) and Sn/Ge(111) (b) systems. It can be observed that the extent of the perturbations originated from defects is much shorter in the Pb/Si(111) surface. The STM image sizes, sample voltages, and tunnel currents are  $11 \times 11 \text{ nm}^2$ ,  $-1.5 \text{ V}$ , and  $0.2 \text{ nA}$  for both (a) and (b).

density of Si defects is so high that the mosaic phase is formed. The behavior of the bias voltage dependent STM images in the Pb/Si(111) mosaic phase has been previously reported<sup>29</sup> and it is in good agreement with the one shown here.

### C. Local perturbation generated from point defects

As stated above, the vast majority of the point defects existent in the Pb/Si(111) surface are substitutional Si adatoms, therefore we have focused on the role played by these defects on the  $\sqrt{3} \leftrightarrow (3 \times 3)$  phase transition. In STM images it can be seen that the presence of substitutional Si adatoms locally modifies the surface. This local perturbation induced by the Si defects can be associated with the existence of the underlying  $\sqrt{3} \leftrightarrow (3 \times 3)$  phase transition. In the isoivalent Sn/Ge(111) system, substitutional defects also create a local perturbation of the surface. For the Sn/Ge(111) system, Melechko *et al.*<sup>5,8,18</sup> have reported that substitutional defects generate an exponentially attenuated modulation with the  $(3 \times 3)$  symmetry characterized by a decay length which was temperature dependent. The extent of these modulations increased when decreasing the temperature, and they found that the inverse of the decay length was linear with temperature. Thus, they proposed that the critical temperature for a defect-free surface would come from the extrapolation of the inverse of this decay length to zero [70 K for the Sn/Ge(111) case] and that the critical temperature experimentally observed was given by the average distance between defects. They also suggest that this analysis could remain valid for other systems where the  $\sqrt{3} \leftrightarrow (3 \times 3)$  phase transition took place.

In the Pb/Si(111) surface, the extent of the perturbation originated from the defects is much shorter than in the Sn/Ge(111) one. As can be observed in Figs. 5(a) and 5(b), where two STM images measured at RT in the Pb/Si(111) (a) and Sn/Ge(111) (b) systems are shown, the extent of the modulations produced by the presence of defects is much

shorter in the Pb/Si(111) case. While at RT in the Pb/Si(111) surface only first neighbors are affected by the presence of the defects [Fig. 5(a)], in the Sn/Ge(111) case even at RT (i.e., more than 200 K above  $T_c$ ) large  $(3 \times 3)$  regions stabilized by the presence of the defects can be observed [Fig. 5(b)]. Moreover, in the Pb/Si(111) system, the temperature dependence of the extent of the perturbations is much smaller than in the Sn/Ge(111) case and, even at 110 K (i.e., only  $\sim 25 \text{ K}$  above  $T_c$ ), the extent of the perturbations originated from defects observed in Pb/Si(111) STM images is shorter than the one found at RT for the Sn/Ge(111) system.<sup>30</sup>

### D. Immobility of point defects from 40 to 300 K

The last point addressed in this work has been the possible existence of a motion of the point defects in the vicinity of the  $\sqrt{3} \leftrightarrow (3 \times 3)$  phase transition. The mobility of substitutional point defects at temperatures near the critical temperature for the  $\sqrt{3} \leftrightarrow (3 \times 3)$  phase transition is quite a controversial issue. For the  $1/3 \text{ ML}$  Sn/Ge(111) system, the existence of a large long-range interaction between defects with the  $(3 \times 3)$  symmetry that forces the substitutional defects to move from the random distribution they present at RT to the alignment onto one honeycomb sublattice with the  $(3 \times 3)$  symmetry found at LT has been reported.<sup>5,8,18</sup> In this way, at LT, substitutional Ge defects were found to preferentially replace Sn<sub>down</sub> adatoms and almost none of them were found in the sites corresponding to Sn<sub>up</sub> adatoms (*down* and *up* subscripts correspond to dark and bright adatoms in filled state STM images, respectively). In order to detect the motion of point defects, these authors performed a complex statistical analysis of STM images measured at different temperatures.<sup>8</sup> It is important to stress that STM images analyzed at different temperatures corresponded to different regions and possibly to different samples. For the Pb/Ge(111) system, it has also been reported<sup>20</sup> that defects should move when the  $\sqrt{3} \leftrightarrow (3 \times 3)$  phase transition takes place and also that a second motion of defects should occur when the temperature is further lowered and a hypothetical different phase transition occurs. However, this latter possibility has already been ruled out by our recent results<sup>15</sup> and the statement that the defects moved throughout the  $\sqrt{3} \leftrightarrow (3 \times 3)$  phase transition was not based on a statistical analysis such as for the Sn/Ge(111) case.<sup>31</sup>

In order to investigate a hypothetical motion of the point defects in the Pb/Si(111) system, we have taken advantage of our ability to vary the sample temperature while tracking the same surface region with atomic resolution.<sup>3,15</sup> We have followed the evolution of the defective regions in a temperature range which extends from temperatures well below  $T_c$  to temperatures well above it, more exactly from 40 to 200 K. To avoid quenching effects, the temperature variation rate has always been slower than  $0.3 \text{ K/min}$  [which is much slower than the  $4 \text{ K/min}$  rate used for the Sn/Ge(111) system<sup>8</sup>]. We have never detected any motion of the point defects in any of the experiments that we have performed. As an example, several pairs of STM images measured on ex-

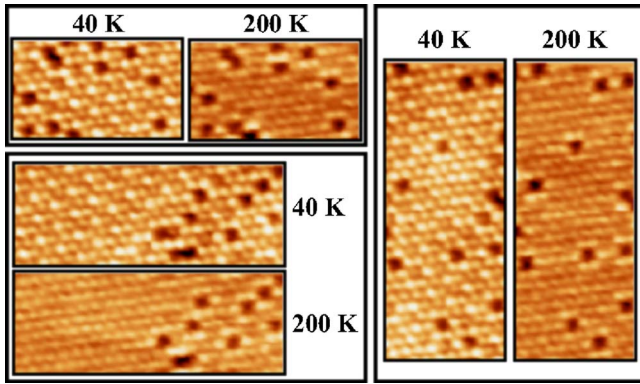


FIG. 6. (Color online) Several pairs of STM images showing exactly the same defective regions of the sample at 40 and 200 K. None of the point defects modifies its position while varying the temperature in such a large range. All the images are measured at a sample voltage of  $-1.5$  V and at a tunnel current of  $0.1$  nA.

actly the same regions at 40 and 200 K are shown in Fig. 6. As can be observed, none of the point defects has varied its position in such a large temperature range. These experiments demonstrate that point defects are not mobile between 40 and 200 K. However, one could question whether the defects could have moved at higher temperatures or even whether the defects are already ordered with the  $(3 \times 3)$  periodicity at RT. In order to check this, we have investigated the correlation between the position of the defects following the statistical analysis performed by Melechko *et al.*<sup>8</sup> We have analyzed STM images<sup>32</sup> measured at RT and at 40 K, and we have found that Si defects are randomly placed both at RT and at 40 K. To perform the statistical analysis, we have chosen a sampling area of  $8 \times 8$  nm<sup>2</sup> that we have used to randomly sample the surface. In Fig. 7 we have plotted the defect distributions obtained for the Pb/Si(111) system at RT (a), at 40 K (c), and for a simulation in which the Si defects have been placed in a random way (b). These defect distributions correspond to the probability of finding a certain amount of Si defects replacing  $Pb_{up}$  adatoms.<sup>33</sup> There exist three possible  $(3 \times 3)$  sublattices that can be generated from

the original  $\sqrt{3}$  lattice. In the statistical analysis,  $Pb_{up}$  adatom sites correspond to the  $(3 \times 3)$  sublattice, which has less defects. Therefore, the amount of Si defects replacing  $Pb_{up}$  adatoms is always  $\leq 33\%$ . We have represented the data grouping them into six bins, each of the bins corresponding to a range of  $33/6\% \approx 5.5\%$ . As can be observed, the distributions obtained for both RT and 40 K are perfectly compatible with the simulated distribution for Si defects in random positions. The value of the first bin of the distributions is especially relevant. It is defined as the correlation probability ( $P_c$ ) and it has the meaning of being the percentage of sampling areas of the surface for which almost none ( $\leq 5.5\%$ ) of the Si defects are replacing  $Pb_{up}$  adatoms or, equivalently, the percentage of sampling areas with almost all Si defects arranged into a honeycomb lattice with the  $(3 \times 3)$  periodicity. Therefore, a low  $P_c$  value corresponds to randomly placed defects, while a high  $P_c$  value corresponds to defects aligned with the  $(3 \times 3)$  periodicity. This correlation probability was the parameter used by Melechko *et al.* to detect the motion of point defects in the Sn/Ge(111) system:<sup>5,8,18</sup> a  $P_c \sim 10\%$  value was found for the RT distribution and a different  $P_c \sim 50\%$  value was found for the low-temperature (50 K) distribution. In the present case, for both the RT and 40 K distributions, this correlation probability is almost negligible, which means that defects are not ordered with the  $(3 \times 3)$  periodicity in the whole temperature range. Therefore, all the results presented here confirm that in the Pb/Si(111) system point defects are immobile and randomly placed from RT to 40 K.

#### IV. SUMMARY AND CONCLUSIONS

By means of variable temperature STM experiments, the role played by substitutional point defects in the  $\sqrt{3} \leftrightarrow (3 \times 3)$  phase transition that take place in the Pb/Si(111) system has been investigated. It has been shown that it is possible to grow extremely large defect-free regions which coexist with more defective ones. The point defects existent in the defective regions have been characterized, finding that most of them ( $\sim 90\%$ ) are substitutional Si adatoms. The

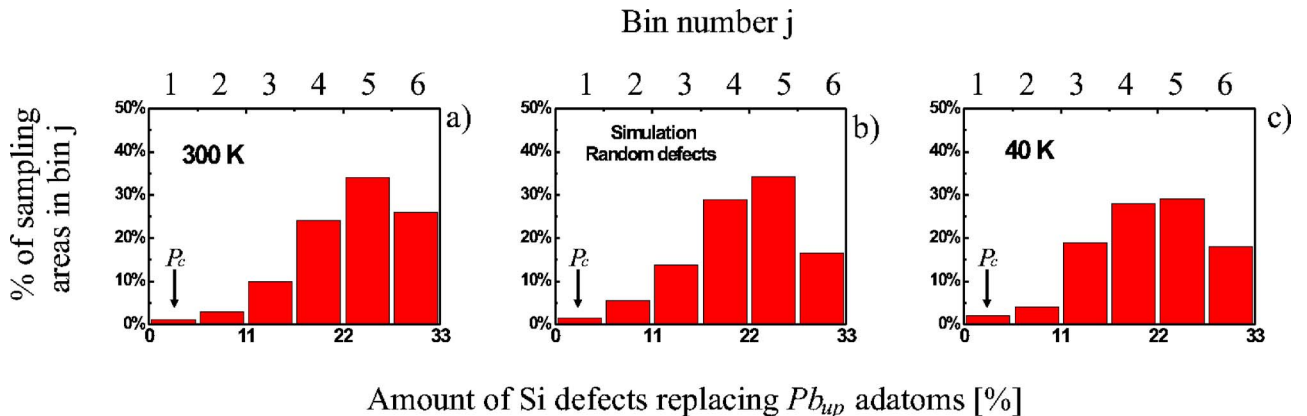


FIG. 7. (Color online) Defect distributions showing the probability of finding a certain amount of Si defects in  $(3 \times 3)$   $Pb_{up}$  adatom sites. (a) and (c) Results for the analysis of STM images measured at 300 K (a) and 40 K (c). (b) Distribution obtained from a simulated  $\sqrt{3}$  surface with randomly placed defects. The first bin of each distribution, marked with an arrow, corresponds to the correlation probability  $P_c$  (see text).

perturbation generated by the Si defects is more localized and has a less noticeable temperature dependence compared to the Sn/Ge(111) system. Finally, we have demonstrated that point defects are immobile and randomly distributed from 40 K to RT.

## ACKNOWLEDGMENTS

We thank A. Cano and A. Levanyuk for fruitful discussions. Financial support from Spain's MEC, under Grant No. MAT2004-03129, is gratefully acknowledged.

\*Present address: Max-Planck-Institut für Festkörperforschung, Heisenbergstrasse 1, D-70569 Stuttgart, Germany. Electronic address: ivan.brihuega@uam.es

- <sup>1</sup>J. M. Carpinelli, H. H. Weitering, E. Ward Plummer, and R. Stumpf, *Nature (London)* **381**, 398 (1996).
- <sup>2</sup>J. M. Carpinelli, H. H. Weitering, M. Bartkowiak, R. Stumpf, and E. W. Plummer, *Phys. Rev. Lett.* **79**, 2859 (1997).
- <sup>3</sup>I. Brihuega, O. Custance, R. Pérez, and J. M. Gómez-Rodríguez, *Phys. Rev. Lett.* **94**, 046101 (2005).
- <sup>4</sup>A. Goldoni and S. Modesti, *Phys. Rev. Lett.* **79**, 3266 (1997).
- <sup>5</sup>A. V. Melechko, J. Braun, H. H. Weitering, and E. W. Plummer, *Phys. Rev. Lett.* **83**, 999 (1999).
- <sup>6</sup>J. Ávila, A. Mascaraque, E. G. Michel, M. C. Asensio, G. Le Lay, J. Ortega, R. Pérez, and F. Flores, *Phys. Rev. Lett.* **82**, 442 (1999).
- <sup>7</sup>A. Mascaraque, J. Ávila, J. Álvarez, M. C. Asensio, S. Ferrer, and E. G. Michel, *Phys. Rev. Lett.* **82**, 2524 (1999).
- <sup>8</sup>A. V. Melechko, J. Braun, H. H. Weitering, and E. W. Plummer, *Phys. Rev. B* **61**, 2235 (2000).
- <sup>9</sup>R. Pérez, J. Ortega, and F. Flores, *Phys. Rev. Lett.* **86**, 4891 (2001).
- <sup>10</sup>O. Custance, J. M. Gómez-Rodríguez, A. M. Baró, L. Jure, P. Mallet, and J. Y. Veuillen, *Surf. Sci.* **482-485**, 1399 (2001).
- <sup>11</sup>G. Ballabio, G. Profeta, S. de Gironcoli, S. Scandolo, G. E. Santoro, and E. Tosatti, *Phys. Rev. Lett.* **89**, 126803 (2002).
- <sup>12</sup>J. Ortega, R. Pérez, and F. Flores, *J. Phys.: Condens. Matter* **14**, 5979 (2002); L. Petersen, Ismail, and E. W. Plummer, *Prog. Surf. Sci.* **71**, 1 (2002), and references therein.
- <sup>13</sup>D. Fariás, W. Kamiński, J. Lobo, J. Ortega, E. Hulpke, R. Pérez, F. Flores, and E. G. Michel, *Phys. Rev. Lett.* **91**, 016103 (2003).
- <sup>14</sup>J. Shi, B. Wu, X. C. Xie, E. W. Plummer, and Z. Zhang, *Phys. Rev. Lett.* **91**, 076103 (2003).
- <sup>15</sup>I. Brihuega, O. Custance, M. M. Ugeda, N. Oyabu, S. Morita, and J. M. Gómez-Rodríguez, *Phys. Rev. Lett.* **95**, 206102 (2005).
- <sup>16</sup>T. L. Lee, S. Warren, B. C. C. Cowie, and J. Zegenhagen, *Phys. Rev. Lett.* **96**, 046103 (2006).
- <sup>17</sup>M. Dávila, J. Ávila, M. C. Asensio, M. Góthelid, U. O. Karlsson, and G. Le Lay, *Surf. Sci.* **600**, 3154 (2006).
- <sup>18</sup>H. H. Weitering, J. M. Carpinelli, A. V. Melechko, J. Zhang, M. Bartkowiak, and E. Ward Plummer, *Science* **285**, 2107 (1999).
- <sup>19</sup>S. T. Jemander, N. Lin, H. M. Zhang, R. I. G. Uhrberg, and G. V. Hansson, *Surf. Sci.* **475**, 181 (2001).
- <sup>20</sup>J. Guo, J. Shi, and E. W. Plummer, *Phys. Rev. Lett.* **94**, 036105 (2005).
- <sup>21</sup>R. Cortés, A. Tejada, J. Lobo, C. Didiot, B. Kierren, D. Malterre, E. G. Michel, and A. Mascaraque, *Phys. Rev. Lett.* **96**, 126103 (2006).
- <sup>22</sup>O. Custance, S. Brochard, I. Brihuega, E. Artacho, J. M. Soler, A. M. Baró, and J. M. Gómez-Rodríguez, *Phys. Rev. B* **67**, 235410 (2003).
- <sup>23</sup>All the STM data were acquired and processed with WSxM, a free software downloadable from <http://www.nanotec.es>. See I. Horcas, R. Fernández, J. M. Gómez-Rodríguez, J. Colchero, J. Gómez-Herrero, and A. M. Baró, *Rev. Sci. Instrum.* **78**, 013705 (2007).
- <sup>24</sup>E. Ganz, I. S. Hwang, F. Xiong, K. Theiss, and J. Golovchenko, *Surf. Sci.* **257**, 259 (1991).
- <sup>25</sup>S. Brochard, E. Artacho, O. Custance, I. Brihuega, A. M. Baró, J. M. Soler, and J. M. Gómez-Rodríguez, *Phys. Rev. B* **66**, 205403 (2002).
- <sup>26</sup>K. Horikoshi, X. Tong, T. Nagao, and S. Hasegawa, *Phys. Rev. B* **60**, 13287 (1999).
- <sup>27</sup>J. Slezák, P. Mutombo, and V. Cháb, *Phys. Rev. B* **60**, 13328 (1999).
- <sup>28</sup>F. Ronci, S. Colonna, S. D. Thorpe, A. Cricenti, and G. Le Lay, *Phys. Rev. Lett.* **95**, 156101 (2005).
- <sup>29</sup>J. M. Gómez-Rodríguez, J. Y. Veuillen, and R. C. Cinti, *Surf. Sci.* **377-379**, 45 (1997).
- <sup>30</sup>I. Brihuega *et al.* (unpublished).
- <sup>31</sup>Indeed, our more recent experiments show that point defects in the Pb/Ge(111) system are also immobile from RT to 40 K [I. Brihuega *et al.* (unpublished)].
- <sup>32</sup>The analysis has been performed using the code written in A. V. Melechko, Ph.D. thesis, The University of Tennessee, 2001.
- <sup>33</sup>For a more detailed explanation of the method, the interested reader is referred to Ref. 8.